

Groundwater quality assessment in Oropos–Kalamos basin, Attica, Greece

G. Stamatis · D. Alexakis · D. Gamvroula ·
G. Migiros

Received: 10 November 2009 / Accepted: 7 January 2011 / Published online: 22 January 2011
© Springer-Verlag 2011

Abstract Groundwater samples were collected from 25 sampling sites of the Oropos–Kalamos basin aiming to describe the groundwater quality in relation to geology, lithology and anthropogenic activities of the study area. Chromium speciation analysis, factor analysis, GIS database and geochemical data proved successful tools for the identification of natural and anthropogenic factors controlling the geochemical data variability and for the identification of the redox couple controlling Cr speciation. A Durov diagram is used to classify groundwater quality into five types: Ca–HCO₃, Mg–HCO₃, Na–Cl, Mg–Cl and Ca–Cl. The groundwater quality of Oropos–Kalamos is influenced by various natural and anthropogenic factors. Evaluation of water quality for drinking and irrigation purposes is discussed.

Keywords Groundwater quality · Arsenic · Chromium speciation · Uranium · Oropos · Attica · Greece

Introduction

Variation in the quality of water resources is related to the presence and concentrations of contaminants, especially

trace elements such as As, Cr, U and V. The global goal of ensuring that human beings have access to acceptable quality water and sufficient quantity faces a number of challenges for the years to come. Urbanization, population mobility, population growth, natural hazards and lately the anticipated climate change are expected to make matters worse in many parts of the globe (Nalbantis and Tsakiris 2009; Tsakiris et al. 2009). Groundwater quality, including both major ionic species and trace elements, strongly influence the management of water resources, as well as their suitability for domestic, agricultural and industrial uses. Human consumption of poor water quality can lead to different kinds of health problems, while the use of poor quality water for irrigation reduces crop productivity. Major and trace element contents of groundwaters utilized for drinking water or irrigating water purposes must be closely monitored. Interactions among water–rock–sediment–soil and the mineral composition of the aquifer materials through which water moves play an important role in groundwater chemistry variation and groundwater quality variation. Furthermore, groundwater quality is often degraded by anthropogenic activities (Arumugam and Elangovan 2009; Espinosa et al. 2009; Fehdi et al. 2009; Kelepertsis et al. 2006; Lambrakis 2006; Stamatis and Gartzos 1999; Skeppstrom and Olofsson 2007; Simsek 2008; Liou et al. 2009).

In the present study, an environmental quality assessment is reported for Oropos–Kalamos groundwaters. The objectives of this paper are: (a) to characterize the groundwater quality of the Oropos–Kalamos basin; (b) to determine the natural and anthropogenic influences on groundwater quality; and (c) to compare element groundwater concentrations in Oropos–Kalamos basin to values established by the European Community, the World Health Organization and the Canadian Council of Ministers of the Environment.

G. Stamatis · D. Gamvroula · G. Migiros
Institute of Mineralogy-Geology,
Agricultural University of Athens,
Iera Odos 75, 118 55 Athens, Greece

D. Alexakis (✉)
Laboratory of Reclamation Works and Water Resources
Management and Centre for the Assessment of Natural Hazards
and Proactive Planning, National Technical University of
Athens, 9 Iroon Polytechniou, 157 73 Athens, Greece
e-mail: dial@survey.ntua.gr

Study area

Geomorphological setting

The study area is situated within the northeastern part of the Attiki region, Greece (Fig. 1), and covers about 800 km². The Oropos–Kalamos basin is located about 50 km north of Athens, the capital of the Greek Republic (Fig. 1). It includes the cities of Oropos, Markopoulo and Kalamos and the villages of Skala Oropou, Nea Palatia, Asprochori, Milesi, Mavrosouvala and Agioi Apostoloi. The area studied extends from the southern Evoikos coastline in the north to the Beletsi hills in the south, from the Oropos city in the west to the Ag.Apostoloi village in the east (Fig. 1). The area studied lies between latitudes 38°14' and 38°20' and longitudes 23°44' and 23°55'.

Morphologically, the study area can be separated into two sections, namely flat and hilly. The Oropos–Markopoulo

plain with an altitude ranging from 20 to 140 m is situated in the northern part of the area (Fig. 1). The hills of Beletsi, Saloniki, Liopesi, Maliza, Spilia Gouri, Mavrinoira and Kamari, with an altitude ranging from 220 to 860 m, are located in the central and southeastern part of the area, and the Kotroni hill with an altitude varying between 0 and 160 m is situated in the northern part of the area (Fig. 1).

Geology and lignite deposits

The geological structure of the study area, which is part of the Pelagonian zone, is dominated by three main units (Fig. 2): (a) the crystalline basement rocks; (b) the alpine basement rocks; and (c) the post-alpine sediments. The crystalline basement rocks are composed of Paleozoic metamorphic rocks (schists, schists with psammitic rocks, schists with marbles and siphiline intercalations). The alpine basement rocks are composed of Mesozoic

Fig. 1 Geomorphological relief of Oropos–Kalamos area and groundwater sampling sites

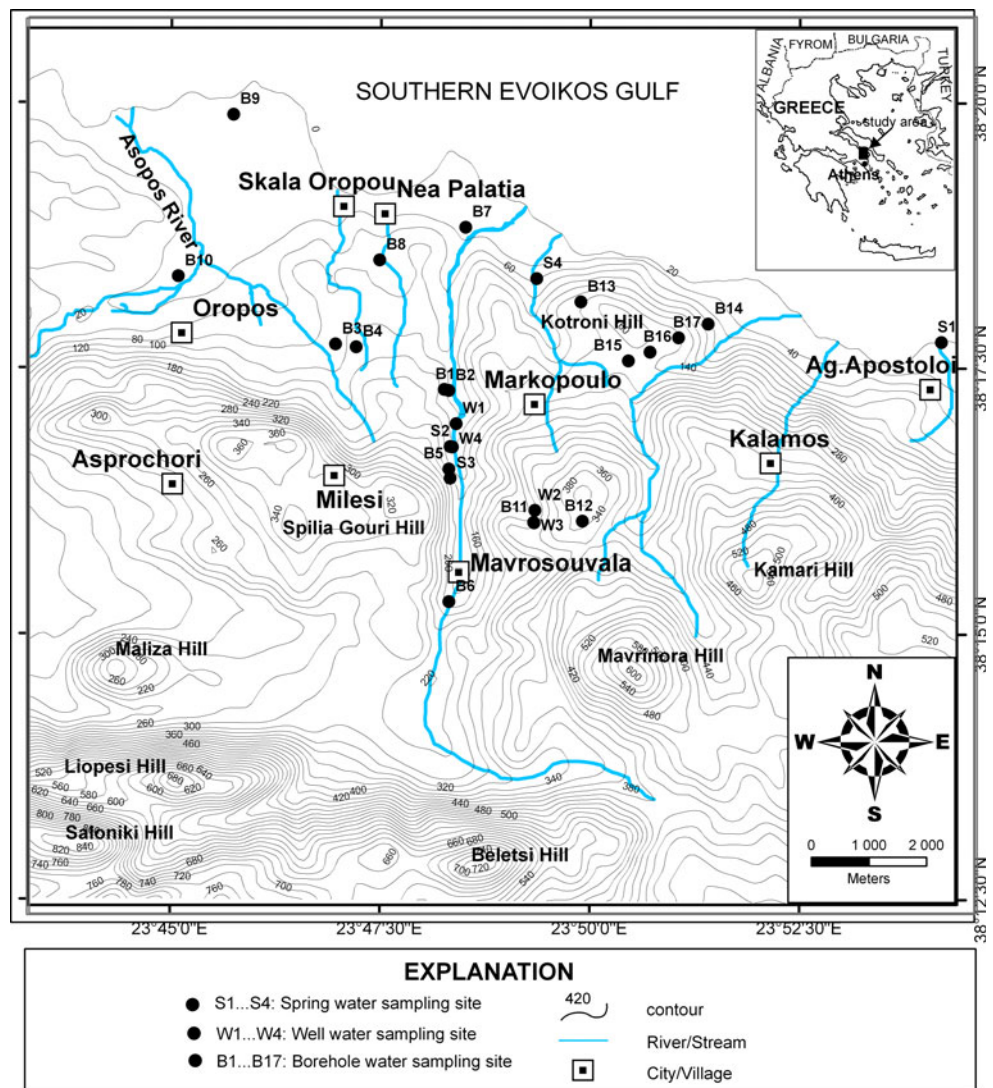
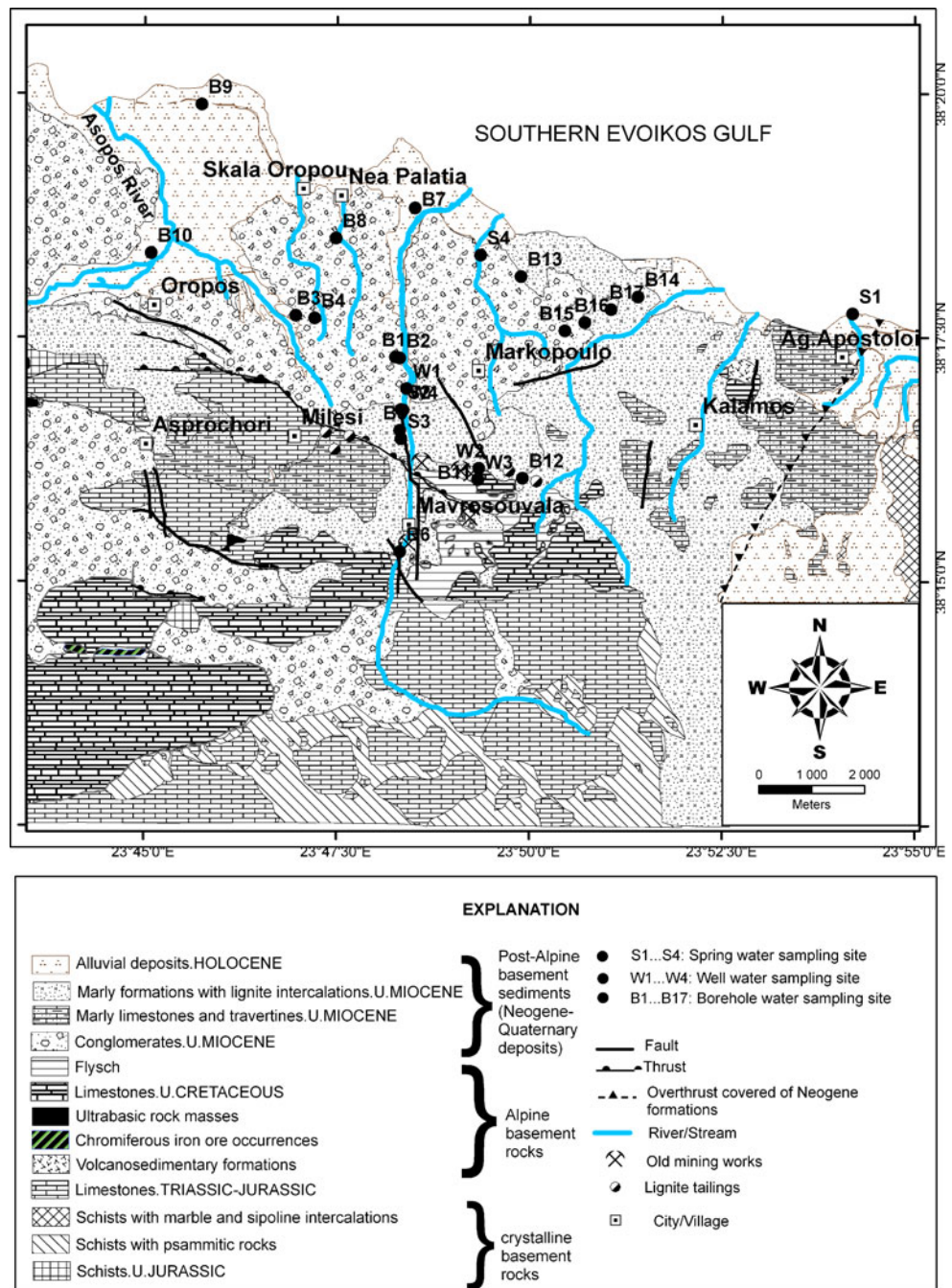


Fig. 2 A simplified geological map of the Oropos–Kalamos area (IGME 2000; Voreadis 1952), showing Oropos–Kalamos groundwater sampling sites



carbonate rocks (limestones and dolomites of Triassic and Jurassic age). Bodies of ultrabasic rocks are locally preserved over the carbonate platform, which were tectonically emplaced during the paleoalpine orogeny of Late Jurassic–Early Cretaceous (IGME 2000; Papanikolaou et al. 1988; Pe-Piper and Piper 2002). The Mesozoic carbonate rocks are covered by Upper Cretaceous shallow water carbonates and early Tertiary flysch, which belong to the geotectonic unit of eastern Greece. Chromiferous iron ore occurrences are covered by Upper Cretaceous limestones (Voreadis 1952). Volcanosedimentary formations

consist of oceanic areas as radiolarites, shales and micritic limestones with silex layers. They are occasionally accompanied by organogenic limestone submarine extrusions of basic eruptive rocks mainly basalts (IGME 2000).

The post-alpine sediments consist mainly of Neogene lignite-bearing deposits, marly formations with lignite intercalations, conglomerates, marly limestones and travertines, and other coarse unconsolidated material (IGME 2000; Papanikolaou et al. 1988).

The lignite deposits of the Oropos–Kalamos basin occur in the Upper Miocene horizon. Lignite in the Mavrosouvala

area occurs as lens intercalations, with thicknesses varying between 1.5 and 12 m, while in the Milesi area it occurs as bed intercalations, with thicknesses of up to 1.5 m (Fig. 2) (Voreadis 1952). Moreover, Voreadis (1952) reported that the lignite deposits of the Oropos area are about 4.3 million metric tons.

Hydrogeology

The Triassic–Jurassic limestones, Upper Cretaceous limestones and marly limestones and travertines are permeable rocks that constitute the most important aquifers of the study area (Fig. 2). The Triassic–Jurassic limestone occurs at the southern part of the study area. The Triassic–Jurassic limestone karstic aquifer outlets are submarine springs and coastal springs located in the Ag.Apostoloi area.

The Upper Miocene conglomerates form a poor aquifer. The boreholes drilled through the conglomerates have discharges varying between 20 and 30 m³ h⁻¹. Groundwater in the conglomerates is recharged by the direct infiltration of rainwater, as well as by the lateral seepage of Asopos River water and the lateral infiltration of water that follows the slope of the Triassic–Jurassic limestone layers into the conglomerates. The marly formations with lignite intercalations form a poor aquifer with discharges ranging up to 20 m³ h⁻¹.

The alluvial deposits form a phreatic aquifer possessing low hydraulic characteristics. The phreatic aquifer feeds a large number of wells and boreholes with depths varying between 10 and 20 m and discharge ranging up to 20 m³ h⁻¹. The hydraulic connection of the alluvial deposits aquifer with the sea in combination with the intensive exploitation for irrigation purposes have contributed to the deterioration of the groundwater quality.

The study area is drained mainly by the tributaries of Asopos River and by six principal seasonal streams, which join the sea along the southern coast of the Southern Evoikos Gulf (Fig. 1). The Asopos River has high flows during autumn and winter and low flows during spring and summer. In contrast, the six seasonal streams are dry for many months of the year.

Anthropogenic activities in the Oropos–Kalamos basin

The land in Oropos, Skala Oropou, Nea Palatia, Asprochori, Markopoulo, Kalamos and Ag.Apostoloi area is characterized by intensive agricultural activities, especially vineyards, vegetables and olive oil trees. In the past, the Oropos–Kalamos basin was one of the most important lignite-bearing areas in Greece.

The Oropos–Kalamos lignite deposits have been exploited since 1870 and have played an important role in meeting the mineral fuel requirements of Greece (Voreadis

1952). In the past, the most important lignite mines of Oropos–Kalamos basin were those of Mavrosouvala and Milesi (Fig. 2). During World Wars I and II, the Mavrosouvala and Milesi mines were operating intensively, but since 1966 there has been no lignite mining activity within the basin. Moreover, great amounts of waste produced from lignite mining activities were deposited in piles around Milesi and Mavrosouvala areas. The water quality of the Asopos River, which runs through many industrial areas, is heavily influenced by the direct discharge of industrial wastewater and wastewater effluents from villages and towns.

Materials and methods

Sampling, preparation and field work

The sampling plan for this study was designed to collect site-specific information related to the influences of industrial and agricultural activities near the sampling sites. Measurement of temperature, dissolved oxygen (O₂), pH, Eh, total dissolved solids (TDS) and electric conductivity (CND) was performed in the field at the time of groundwater sampling with a WTWTM 350i multifunction portable meter. The locations of groundwater sampling sites were recorded in the field using a Garmin eMap Geographical Positioning System (GPS). A single round of water samples was collected from 25 locations within the study area during July–August 2008 (Fig. 1). Water samples were collected from the surface discharges of existing springs and from agricultural, domestic wells, public water-supply wells and boreholes and placed into pre-cleaned polypropylene containers, which were rinsed three times with sample water prior to sample collection. Each water sample was then divided into four water subsamples. One set of 25 subsamples was vacuum filtered through 0.45-μm pore size membrane filters and stored in 1,000 mL container for major cation and anion analyses. The second set of 25 subsamples was filtered with sterile 0.22-μm disposable syringe filter and acidified to pH < 2 with about 1 mL ultrapure HNO₃ and stored in 100-mL container for trace element analysis. The other two sets of subsamples were separated in the field by the cation-exchange method described by Ball and McCleskey (2003). The third set of subsamples was filtered with an assembly of plastic syringe/sterile 0.22-μm disposable filter and acidified to pH < 2 with 10 μL HNO₃ and stored in 2-mL centrifuge tube for Cr_{total} analysis. The fourth set of subsamples was forced through a cation-exchange cartridge (IC-H, Alltech) and an assembly of plastic syringe/0.22 μm disposable filter and acidified to pH < 2 with 10 μL HNO₃ and stored in 2-mL centrifuge tube for Cr⁶⁺ analysis.

The different oxidation states of Cr in groundwater can be unstable and may oxidize when exposed to air. Thus, concentrations of the respective redox states should be determined at the time of sampling or separated from each other in the field and preserved for later analysis in the laboratory (Ball and Izbicki 2004). The cation-exchange Cr speciation method applied in this study has been demonstrated by Ball and Izbicki (2004) to be the simplest to use in the field and is equivalent to USEPA method 218.6 in accuracy and sensitivity.

All possible precautions were taken during collection and handling of water samples to minimize contamination. All the water subsamples were stored in an iced cooler during the fieldwork. The temperature of water samples stored in the fridge in the laboratory was maintained at a temperature between 2 and 4°C.

Chemical analysis

Dissolved anions, including NH_4^+ -N, NO_3^- -N, PO_4^{3-} -P and SO_4^{2-} , were measured photometrically for the non-acidified samples using a HACH DR 3000 apparatus, while bicarbonate (HCO_3^-) was measured using a HACH digital titrator at the Laboratory of Geology of the Agricultural University of Athens. To measure Cl^- and total hardness (H_{total}), titration methods were applied using Titriplex-Losung A 0.1 M AgNO_3 and 0.1 M HCl, respectively (Hoell 1979).

Chromium total (Cr_{total}) and chromium hexavalent (Cr^{+6}) chemical analysis was performed by using atomic absorption spectroscopy (AAS/Perkin Elmer 1100B) with a Graphite Furnace at the Laboratory of Economic Geology and Geochemistry of the National and Kapodistrian University of Athens.

Trace elements including: Ag, Al, As, Au, B, Ba, Be, Bi, Br, Cd, Ce, Co, Cr_{total} , Cs, Cu, Dy, Er, Eu, Fe, Ga, Gd, Ge, Hf, Hg, Ho, In, Ir, La, Li, Lu, Mn, Mo, Nb, Nd, Ni, Os, P, Pb, Pd, Pr, Pt, Rb, Re, Rh, Ru, S, Sb, Sc, Se, Si, Sm, Sn, Sr, Ta, Tb, Te, Th, Ti, Tl, Tm, U, V, W, Y, Yb, Zn and Zr were analyzed by inductively coupled plasma mass spectroscopy (ICP-MS) at the ACME Analytical Laboratories Ltd, Vancouver, Canada (ISO 9002 Accredited Co.).

Dissolved cations, including Ca^{2+} and Mg^{2+} , were measured for the non-acidified set of subsamples by atomic absorption spectroscopy (AAS/GBC 908 AA), while Na^+ and K^+ were measured using flame photometry (INTECH/1382) at the Laboratory of Geology of the Agricultural University of Athens.

The charge-balance error for major ionic species, calculated using Microsoft Excel and the software package AQUACHEM, did not exceed 5%. Total chromium measurements (Cr_{total}) from the two laboratories (National University of Athens and ACME) were compared and

found to have <5% difference between their analytical results.

Statistical analysis and use of GIS

For the statistical analysis, 21 chemical parameters were selected on the basis of specific interest related to the type of anthropogenic activities and lithology of the study area.

Statistical software codes (Microsoft® Excel, MINITAB® and SPSS®) were used to study the geochemical data distribution and the relationships between water quality parameters within the Oropos–Kalamos basin. The univariate summary statistics of the Oropos–Kalamos groundwater geochemical data set were calculated. Saturation indices (SI) for selected minerals were calculated using the software code AQUACHEM to better understand the hydrochemical processes that take place in the aquifers.

The saturation indices are expressed as $\text{SI} = \log(\text{IAP}/\text{K})$, where IAP is the ion activity product and K is the equilibrium solubility constant. If the solution is saturated in a mineral, the $\text{SI} > 0$ and the mineral tend to precipitate, while if the solution is unsaturated in a mineral, the $\text{SI} < 0$ and the mineral would tend to dissolve. If the solution is in equilibrium with a mineral, then $\text{SI} = 0$.

The log-transformed geochemical data set (21×25) was processed by the R-mode factor analysis, applying the Varimax-raw rotational technique with Kaiser normalization, to separate and identify the distributions associated with individual components. The correct number of factors was selected by using a combination of the common criteria (Davis 1986; Alexakis and Keleperdis 1998; Stamatis et al. 2006). Factor loadings were calculated using an eigenvalue greater than 1.

For the purposes of determining inter-element relationships, factor loadings between 0.50 and 0.75 were defined as “moderate”, loadings >0.75 were defined as “high”, and loading <0.5 were defined as “low”. Negative factor scores indicate areas that are unaffected by either natural or anthropogenic processes, and positive scores indicate the areas that are most affected by hydrochemical processes. Near-zero values suggest an average effect by all hydrochemical processes. Simplified digital geochemical maps were created using ArcGIS 9.3 software (ESRI). Two topographic maps of scale 1:50,000 from the Greek Geographical Military covering the study area and including the sampling sites were scanned. All maps required georeferencing to the area coordinates according to the HGRS 87. Geological formations, faults and thrusts were obtained by digitizing the scanned and georeferenced geological maps of IGME (2000) and Voreadis (1952). The scanned and georeferenced images of topographic and geological maps were inserted in GIS as the basic layers, showing the locations of lithology, streams and cities. The

element concentrations and the factor scores were projected on the digital map using graduated size symbols.

Results

Table 1 presents the univariate statistics summary ($n = 25$) for 45 water quality parameter values, hardness total

(H_{total}), TDS, Eh, pH and conductivity (CND) values along with the corresponding parametric values (PVs) given by the Council Directive 98/83/EC (EC 1998).

The elements Ag, Au, Be, Bi, Dy, Er, Eu, Ga, Gd, Ge, Hf, Hg, Ho, In, Ir, Lu, Nb, Nd, Os, Pd, Pr, Pt, Rh, Ru, Sm, Ta, Tb, Te, Th, Ti, Tl, Tm, W, Y, Yb and Zr in all groundwater samples ($n = 25$) were not detected. The temperature value of the Oropos–Kalamos groundwater

Table 1 Univariate statistics summary of Oropos–Kalamos groundwater physicochemical parameter data set ($n = 25$) in comparison with PVs and WQLs obtained by literature

	Units	DL	Min	Max	Mean	Median	SD	PV ^a	PPPV ^b (%)	WQL ^c	PPWQL ^d (%)
Al	µg L ⁻¹	1	1	17	5	4	3	200	0	5,000	0
As	µg L ⁻¹	0.5	0.5	246.5	23.3	2.8	53.5	10	32	100	8
B	µg L ⁻¹	5	6	533	67	43	103	1,000	0	500	4
Ba	µg L ⁻¹	0.05	11.01	181.21	67.63	65.60	46.61	–	–	–	–
Br	µg L ⁻¹	5	57	10,102	658	193	1,977	–	–	–	–
Ca	mg L ⁻¹	0.05	79.04	362.05	131.30	111.31	59.59	–	–	–	–
Cd	µg L ⁻¹	0.05	0.05	0.50	0.07	0.05	0.09	5	0	5.1	0
Ce	µg L ⁻¹	0.01	0.01	0.11	0.02	0.01	0.03	–	–	–	–
Cl	mg L ⁻¹	1	24	2908	239	106	562	250	16	–	–
Co	µg L ⁻¹	0.02	0.03	0.91	0.15	0.06	0.22	–	–	50	0
Cr ⁶⁺	µg L ⁻¹	0.5	1.4	27.9	8.0	1.9	9.3	–	–	8.0	16
Cr _{total}	µg L ⁻¹	0.5	1.2	34.3	7.4	2.0	10.1	50	0	12.9	16
Cs	µg L ⁻¹	0.01	0.01	3.58	0.66	0.12	0.99	–	–	–	–
Cu	µg L ⁻¹	0.1	0.5	15.2	2.9	2.0	3.1	2,000	0	200	0
Fe	µg L ⁻¹	10	10	2,486	193	71	510	200	8	5,000	0
HCO ₃ ⁻	mg L ⁻¹	1	336	641	436	427	75	–	–	–	–
K	mg L ⁻¹	0.05	0.56	58.59	4.57	1.50	11.60	–	–	–	–
La	µg L ⁻¹	0.01	0.01	5.46	0.33	0.06	1.08	–	–	–	–
Li	µg L ⁻¹	0.1	1.0	80.2	20.7	20.4	16.7	–	–	2,500	0
Mg	mg L ⁻¹	0.05	14.82	157.81	52.81	50.47	33.37	–	–	200	0
Mn	µg L ⁻¹	0.05	0.14	132.52	12.26	0.74	31.01	50	8	–	–
Mo	µg L ⁻¹	0.1	0.1	28.3	1.7	0.4	5.6	–	–	10	4
Na	mg L ⁻¹	0.05	8.52	1481.87	105.18	33.63	289.26	200	4	–	–
NH ₄ ⁺	mg L ⁻¹	0.01	0.01	2.71	0.46	0.37	0.52	0.50	20	–	–
Ni	µg L ⁻¹	0.2	0.2	83.5	9.8	3.0	18.1	20	16	200	0
NO ₃ ⁻	mg L ⁻¹	1	2	30	12	10	7	50	0	–	–
O ₂	mg L ⁻¹	0.1	0.1	31.8	9.2	8.8	6.2	–	–	–	–
P	µg L ⁻¹	20	20	200	46	32	39	–	–	–	–
Pb	µg L ⁻¹	0.1	0.1	64.5	3.6	0.8	12.7	10	4	200	0
PO ₄ ³⁻	mg L ⁻¹	0.10	0.10	0.50	0.16	0.11	0.17	–	–	–	–
Rb	µg L ⁻¹	0.01	0.33	19.43	3.14	1.27	4.34	–	–	–	–
Re	µg L ⁻¹	0.01	0.01	0.27	0.03	0.01	0.05	–	–	–	–
S	mg L ⁻¹	1	3	207	29	9	50	–	–	–	–
Sb	µg L ⁻¹	0.05	0.05	0.61	0.14	0.08	0.15	5	0	–	–
Sc	µg L ⁻¹	1	1	10	4	4	3	–	–	–	–
Se	µg L ⁻¹	0.5	0.5	39.2	3.1	1.5	7.6	10	4	20	4
Si	µg L ⁻¹	40	4,422	27,775	13,314	11,970	7,564	–	–	–	–
SiO ₂	mg L ⁻¹	1	8	43	21	19	12	–	–	–	–
Sn	µg L ⁻¹	0.05	0.05	0.50	0.07	0.05	0.09	–	–	–	–

Table 1 continued

	Units	DL	Min	Max	Mean	Median	SD	PV ^a	PPPV ^b (%)	WQL ^c	PPWQL ^d (%)
SO ₄ ²⁻	mg L ⁻¹	1	2	749	79	24	161	250	8	–	–
Sr	μg L ⁻¹	0.01	97.13	1,999.87	603.78	514.15	419.38	–	–	–	–
Ti	μg L ⁻¹	0.01	0.01	0.24	0.03	0.01	0.05	–	–	–	–
U	μg L ⁻¹	0.02	0.02	14.73	2.19	1.50	2.98	–	–	10	4
V	μg L ⁻¹	0.2	0.2	19.4	2.8	1.4	4.1	–	–	100	0
Zn	μg L ⁻¹	0.5	5.1	974.0	92.1	15.5	206.1	–	–	1000	0
H _{total}	mg L ⁻¹ asCaCO ₃	1	18	70	31	26	13	–	–	–	–
TDS	mg L ⁻¹	2	296	973	529	497	199	–	–	–	–
Eh	mV		-55.40	-14.40	-27.35	-24.95	9.73	–	–	–	–
pH			6.77	7.81	7.30	7.25	0.24	6.5–9.5	0	–	–
CND	μS cm ⁻¹	1	539	1769	943	882	72.4	2,500	0	–	–

DL detection limit, SD standard deviation, H_{total} hardness total

^a Parametric values given by the Dir.98/83/EC (EC 1998)

^b Percentage proportion (%) of water samples exceeding PVs

^c Water quality limits for agricultural water uses adapted from the CCME (1999)

^d Percentage proportion (%) of water samples exceeding water quality limits

samples ranges from +13.8 to +20.7°C. Varimax-rotated factor loadings and the proportion of variance explained are presented in Table 2.

Discussion

Evaluation of water quality for drinking and irrigation uses

The Council Directive 98/83/EC (EC 1998) was the basis for the Oropos–Kalamos water quality evaluation for drinking uses. According to the Directive 98/83/EC, each groundwater sample was assessed to be in compliance if all water quality parameters were lower or equal to the PVs given by the European Community (EC 1998) (Table 1).

The concentrations of Al, B, Cd, Cr_{total}, Cu, NO₃⁻ and Sb in groundwater samples collected from the Oropos–Kalamos basin did not exceed the PVs given by the European Community (EC 1998). The percentage proportions of the Oropos–Kalamos groundwater samples with As, Cl, Fe, Mn, Na, NH₄⁺, Ni, Pb, Se and SO₄²⁻ concentrations exceeding the PVs were 32, 16, 8, 8, 4, 20, 16, 4, 4 and 8%, respectively (Table 1). Arsenic concentration of groundwater samples: B1, B9, B13, B16, B17, W1, W4 and S1 exceed the PV (Table 1, Fig. 2). The concentration of Cl in groundwater samples collected from sites B10, B12, S1 and S4 exceeds the PV. The concentration of Fe in groundwater samples collected from the sites B9 and B13 exceeds the PV. Manganese groundwater contents in the sampling sites B9 and B12 exceed the PV. Sodium and Se concentrations in the groundwater collected from sampling

Table 2 Varimax-rotated R-mode factor analysis matrix for log-transformed Oropos–Kalamos groundwater geochemical data set (n = 25), showing factor loading for all factors with eigenvalues >1 (absolute values below 0.200 are not shown)

	Factor 1	Factor 2	Factor 3	Factor 4
As	0.275			0.780
B	0.716	0.479	0.253	0.340
Ca	0.261	0.803	-0.247	
Cl	0.919	0.279		
Cr ⁶⁺			0.938	
Cr _{Total}			0.898	
Cu				
HCO ₃ ⁻	0.294	0.567	0.42	0.497
K	0.785	0.309		0.387
Mg	0.678	0.418	0.403	0.365
Mn				0.889
Na	0.858	0.411		
NO ₃ ⁻			0.509	-0.324
Ni		0.29		0.589
Pb				
Rb	0.537	0.348		0.62
S	0.435	0.86		
Si			0.655	0.509
SO ₄ ²⁻	0.394	0.881		
U		0.744	0.482	0.274
V	0.747		0.358	
Variance explained (%)	42.23	14.69	12.42	7.97

site S1 exceed the PVs. The NH₄⁺ concentration in the groundwater collected from the sampling sites B9, B10, B12, W2 and W4 exceeds the PV. Nickel groundwater

concentration in the sampling sites B5, W1, W2 and W4 exceeds the PV. Only for the sampling site B16, the groundwater Pb content exceeds the PV. The concentration of SO_4^{2-} in groundwater samples W2 and S1 exceeds the PV. Because of the different health effects of Cr_{total} and Cr^{6+} , the current European Community parametric value of $50 \mu\text{g L}^{-1}$ has been questioned. Furthermore, there is not yet an established PV especially for Cr^{6+} .

Despite the U and V toxicity to humans (Orloff et al. 2004; Skeppstrom and Olofsson 2007; Venkataraman and Sudha 2005), the U and V contents in Oropos–Kalamos groundwater were not routinely measured in the past as indicators of water quality. The percentage proportion of the Oropos–Kalamos groundwater samples with U content exceeding the WHO (2004) recommended limit of $15 \mu\text{g L}^{-1}$ concentration in drinking water is 4%, while a recommended limit for V by WHO has not been established yet. The percentage proportion of Oropos–Kalamos groundwater samples with U content exceeding the U concentration of Attica–Greece network given by Kehagia et al. (2007) is 48%. The pH and CNd values in Oropos–Kalamos groundwater ranges from 6.77 to 7.81 and from 539 to $1,769 \mu\text{S cm}^{-1}$, respectively, and does not exceed the PVs.

The basis for the Oropos–Kalamos water quality evaluation for irrigation purpose was the Water Quality Limits for Agricultural Uses adopted from the Canadian Council of Minister of the Environment (CCME 1999). According to CCME (1999), each groundwater sample was assessed

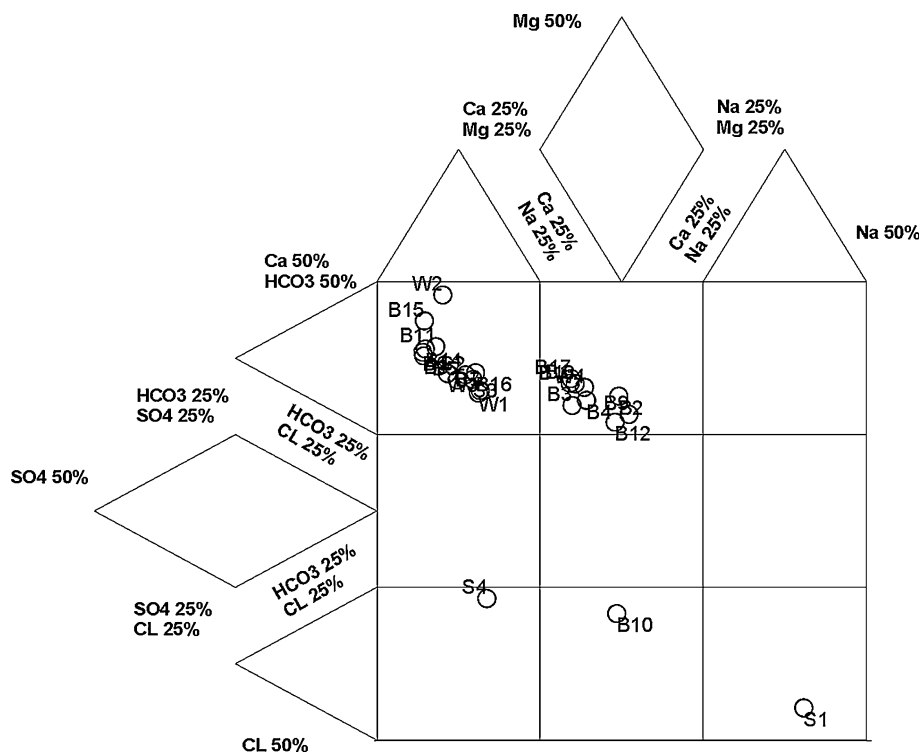
to be in compliance if all water quality parameters did not exceed the water quality limits for agricultural uses (Table 1). The concentrations of Al, Cd, Co, Cu, Li, Mg, Ni, Pb, V and Zn in groundwater samples collected from the Oropos–Kalamos basin did not exceed the water quality limits for agricultural uses given by CCME (1999) (Table 1).

The percentage proportions of the Oropos–Kalamos groundwater samples with As, B, Cr^{6+} , Cr_{total} , Mo, Se and U contents exceeding the Water Quality Limits for Agricultural Uses (CCME 1999) were 8%, 4%, 16%, 16%, 4%, 4% and 4%, respectively (Table 1). Specifically, based on the water quality limits for agricultural uses given by CCME (1999), the groundwater of the sampling sites B1, B2, B3, B4, B10, W2, W4 and S1 is not suitable for irrigation purpose (Fig. 2).

Classification of groundwater

As presented in the expanded Durov diagram (Fig. 3), the Oropos–Kalamos groundwaters are classified into five water types: Ca– HCO_3 , Mg– HCO_3 , Na–Cl, Mg–Cl and Ca–Cl, while the percentage proportions of the Oropos–Kalamos groundwater samples belonging to the water types are 52%, 36%, 4%, 4% and 4%, respectively. The three groundwater samples (S1, S4, B10) that were plotted in fields where Cl is the dominant anion are outliers. The high Cl contents of these groundwater samples are attributed to the mixing of groundwater with seawater. The line

Fig. 3 Classification of groundwater using the expanded Durov diagram for samples from Oropos–Kalamos area



connecting the end members W1 and W2 is plotted in the field where Ca^{2+} and HCO_3^- are the dominant ions. This reflects the dissolution of gypsum, which presents in the water-bearing formations. The line connecting the end members B12 and B17 is plotted in the field where Mg^{2+} and HCO_3^- are the dominant ions. This reflects the dissolution of magnesite, which is present in the water-bearing formations as a weathering product of ultrabasic rock masses.

The mineralogic composition of the water-bearing formations as well as the calculation of thermodynamic equilibrium conditions of Oropos–Kalamos groundwaters showed that the main minerals present in the aquifers are calcite (CaCO_3), aragonite (CaCO_3), anhydrite (CaSO_4), dolomite ($\text{CaMg}(\text{HCO}_3)_2$), gypsum ($\text{CaSO}_4 \cdot 2\text{H}_2\text{O}$) and magnesite (MgCO_3).

Figure 4 shows that the groundwater of the study area is saturated in calcite, aragonite, magnesite and dolomite and unsaturated in gypsum and anhydrite. Therefore, there is a possibility for further Ca^{2+} and SO_4^{2-} concentration increases in the Oropos–Kalamos groundwaters due to the dissolution of gypsum and anhydrite.

Groundwater quality in relation to geology and anthropogenic activities

The spatial distribution of the major and trace ionic species were inspected in the light of known natural and anthropogenic processes. Specifically, the spatial distributions of As, Cr_{total} , Cr^{6+} , U and V in Oropos–Kalamos groundwater were selected on the basis of environmental interest related to lithology and ore composition (these elements have not been studied previously in Oropos–Kalamos groundwater). Moreover, the spatial distributions of As, B, Ca, Cl, Cr^{6+} , Cr_{total} , Cu, HCO_3^- , K, Mg, Mn, Na, NO_3^- , Ni, Pb, Rb, S, Si, SO_4^{2-} , U and V were implicit in the scores of the first, second, third and fourth components of a multivariate analysis (factor analysis) performed on the physicochemical parameter data set of the Oropos–Kalamos groundwater samples.

High As contents (varying between 11 and $247 \mu\text{g L}^{-1}$) were found in groundwater samples collected in an area lying between Kalamos, Markopoulo and Mavrosouvala, especially in the aquifer developed within Marly formations intercalated by lignite and close to the abandoned

Fig. 4 Frequency diagrams for calcite, aragonite, dolomite, magnesite, gypsum and anhydrite saturation indices

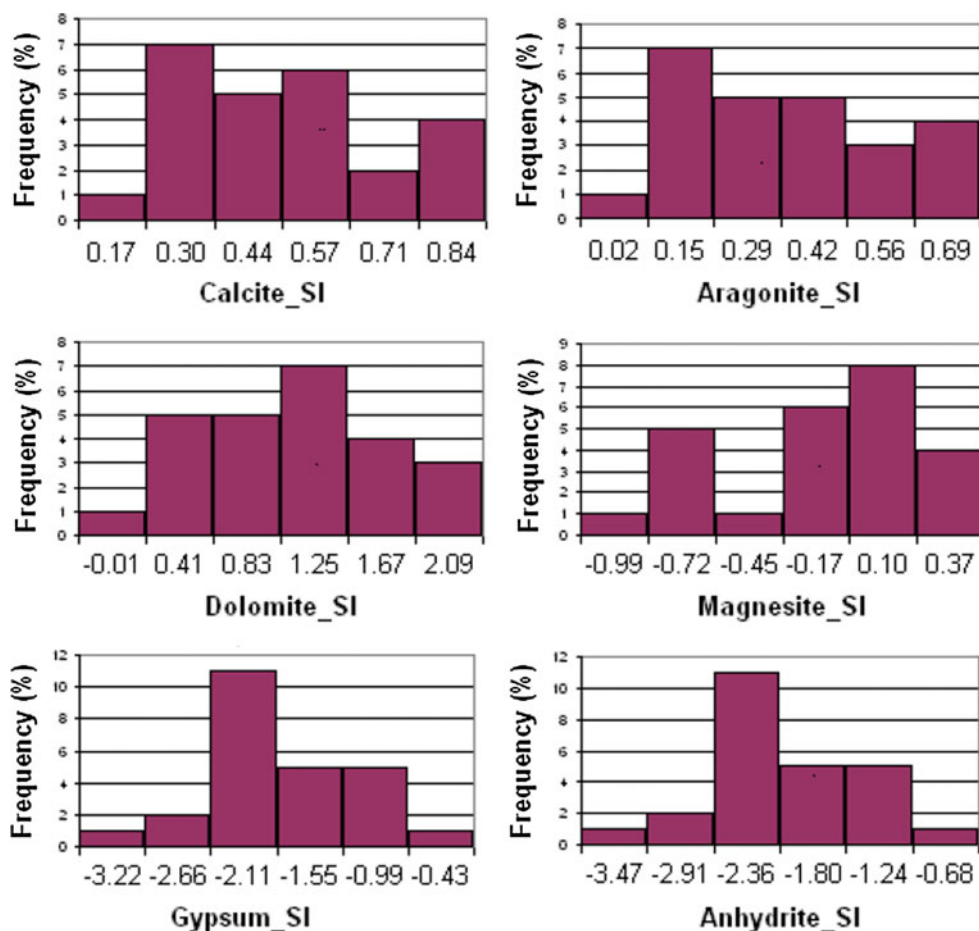
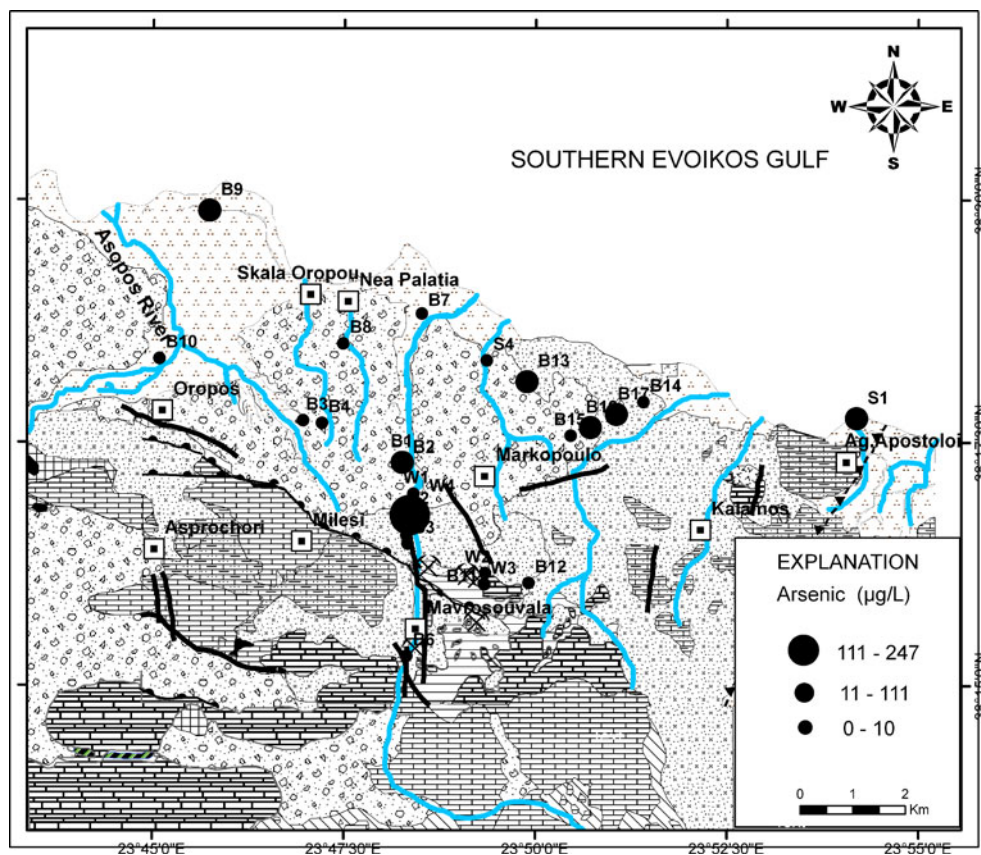


Fig. 5 Symbol map of As groundwater contents in comparison with geology



lignite mining works (see Fig. 5). This suggests that the high As groundwater concentrations are a result of the As contained in lignite intercalations and/or the waste piles that were deposited in the Milesi area. The As contents in groundwater samples collected in the area lying between Oropos and Nea Palatia ranges from 0 to 10 $\mu\text{g L}^{-1}$.

High Cr_{total} concentrations (ranging from 20 to 34 $\mu\text{g L}^{-1}$) occurred in an area between Oropos and Markopoulo, while Cr concentrations in the area that extends east from Markopoulo city vary between 1 and 6 $\mu\text{g L}^{-1}$ (Fig. 6). Because the area between Oropos and Markopoulo is characterized by the absence of industrial activities, the Cr anomalies can be attributed to natural sources, such as the dissolution of ultrabasic rock masses and ultrabasic rock fragments within Neogene and Quaternary deposits.

High Cr^{6+} concentrations (varying between 15 and 28 $\mu\text{g L}^{-1}$) were found in groundwater samples collected in an area between Oropos and Markopoulo; whereas the Cr^{6+} groundwater content of the area that extends east from the Markopoulo city is lower than 3 $\mu\text{g L}^{-1}$ (Fig. 7). The elevated Cr^{6+} values can be attributed to natural sources, such as the oxidation of Cr^{3+} that is released from ultrabasic rock masses and ultrabasic rock fragments within Neogene and Quaternary deposits. A number of other researchers have speculated that high Cr^{6+}

concentrations in groundwater can result from this process. Ball and Izbicki (2004) reported naturally occurring Cr^{6+} concentrations as high as 60 $\mu\text{g L}^{-1}$ in alluvium weathered from metamorphic rocks. Robles-Camacho and Armienta (2000) found up to 12 $\mu\text{g L}^{-1}$ Cr^{6+} in water-bearing ultrabasic rocks, and Fantoni et al. (2002) reported Cr^{6+} concentrations ranging from 5 to 73 $\mu\text{g L}^{-1}$ in similar rock types.

The total U concentration in Oropos–Kalamos groundwater varies from 0.02 to 14.73 $\mu\text{g L}^{-1}$, which greatly exceeds the 0.09–1.40 $\mu\text{g L}^{-1}$ range reported for drinking water in the Attica region of Greece by Kehagia et al. (2007). An anthropogenic origin for elevated U concentrations is discarded because there are no known sources of U contamination in the Oropos–Kalamos basin. Instead, the high U contents of Oropos–Kalamos groundwater can be attributed to natural sources, such as leaching from lignite intercalations. Another case of naturally occurring U in groundwater has been reported by Orloff et al. (2004), who found concentrations ranging from 1.8 to 7,780 $\mu\text{g L}^{-1}$.

Singh et al. (1996) reported the presence of U in groundwater and surface water of some Indian regions as a result of its natural occurrence and also due to man-made activities like mining and milling of lignite and uranium rocks. Moreover, U content for other Greek bulk lignite's samples (varying between 0.1 and 4.1 mg kg^{-1}) has also

Fig. 6 Symbol map of Cr_{total} groundwater contents in comparison with geology

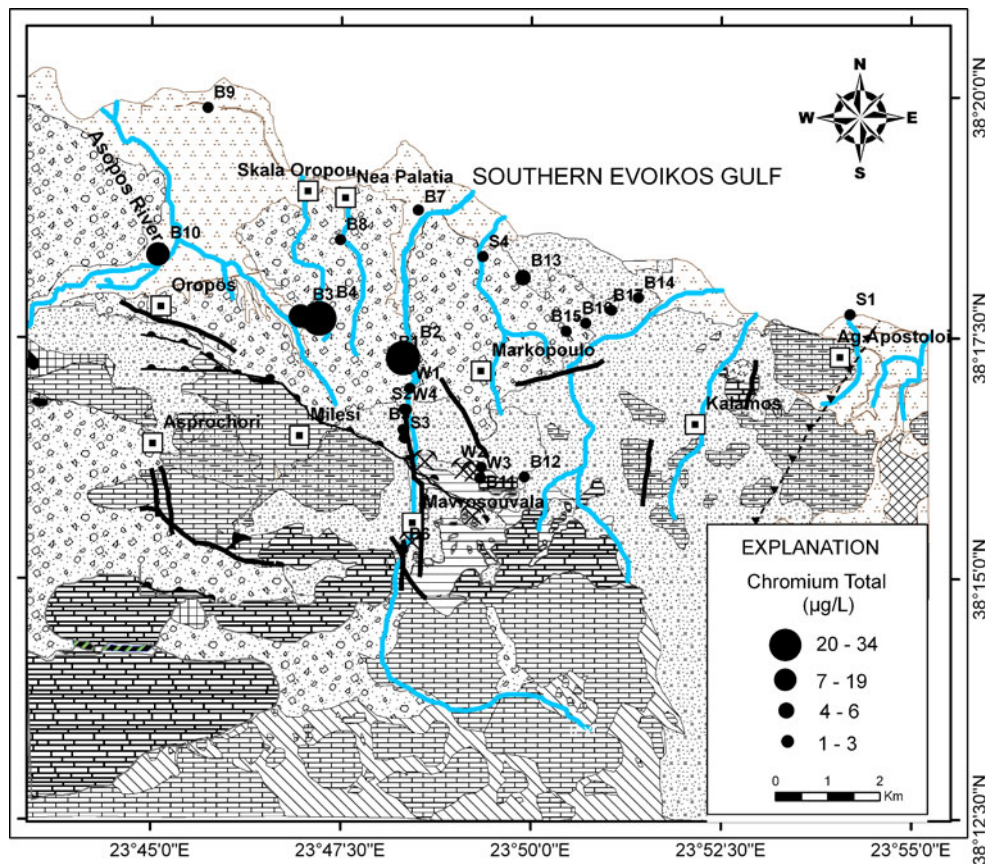


Fig. 7 Symbol map of Cr^{6+} groundwater contents in comparison with geology

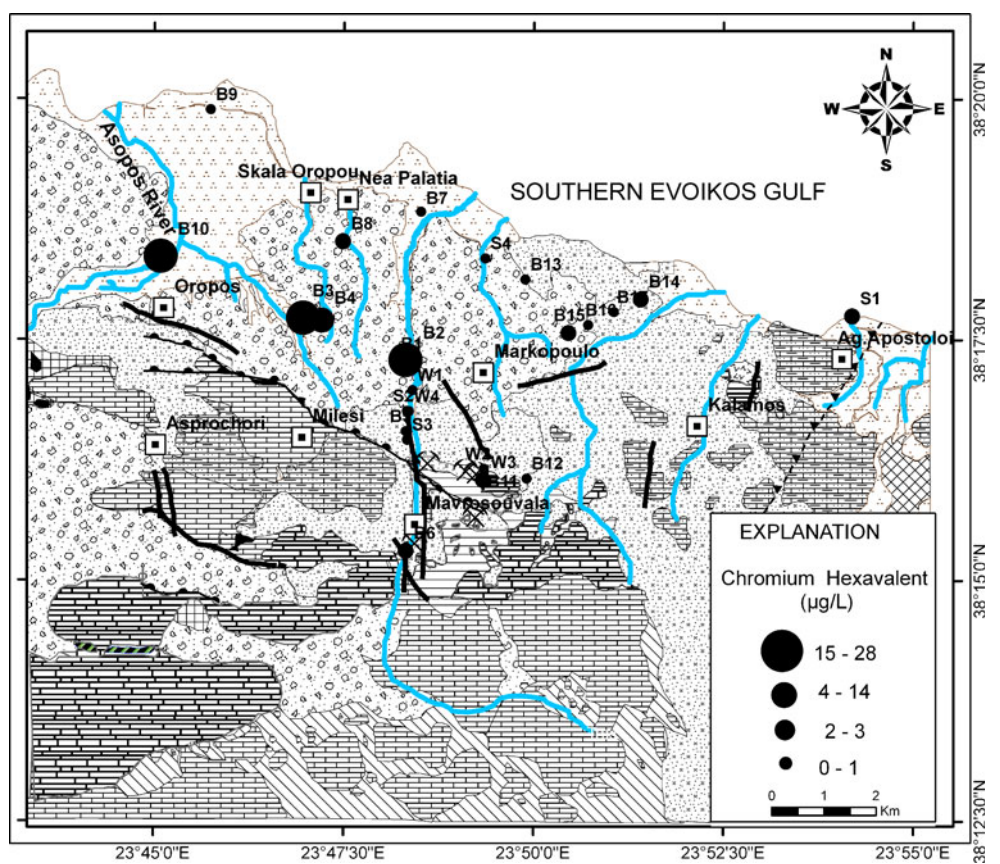
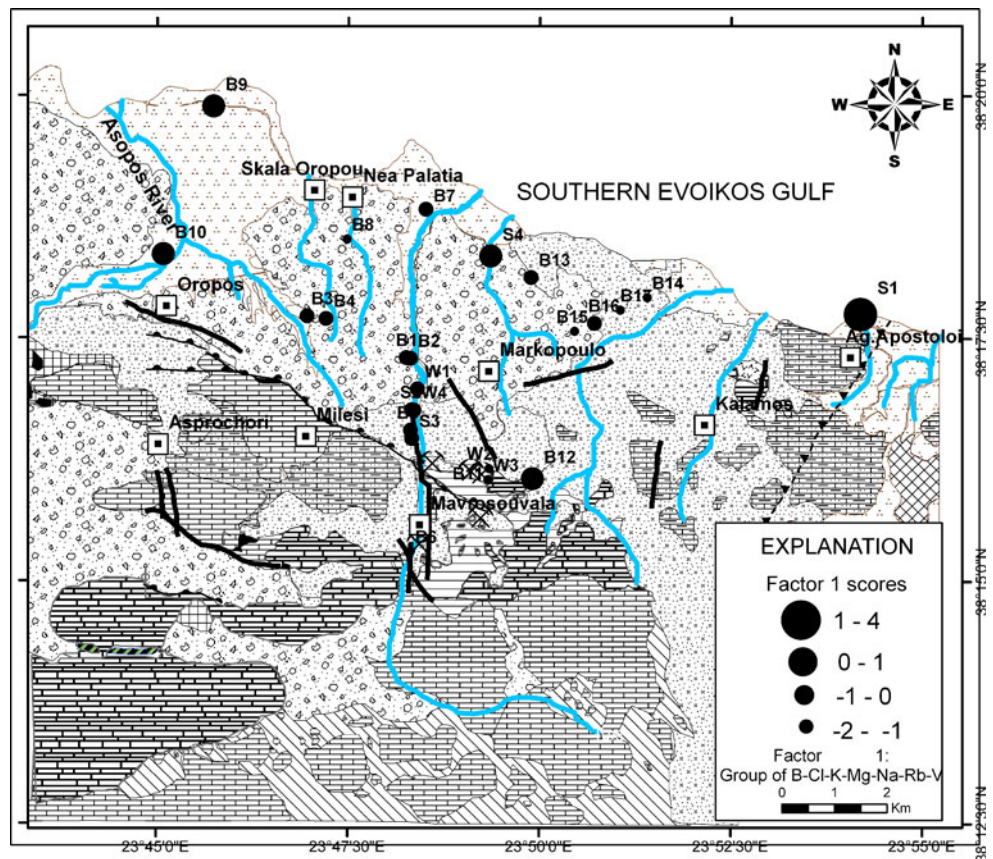


Fig. 8 Graduated symbol plots of Factor 1 scores in comparison with geology



been reported by Chatziapostolou et al. (2006). According to Zamora et al. (1998), the long-term ingestion of groundwater with U content varying between 2 and $781 \mu\text{g L}^{-1}$ affects human kidney function.

In the present study, a four-factor model with a total cumulative variance of 77.41% was obtained (Table 2). Factor 1, which explains the largest proportion (42.23%) of the total variance, has high positive loadings ($>+0.716$) for B, Cl, K, Na and V and median positive loadings for Mg ($+0.678$) and Rb ($+0.537$) (Table 2). The variability of these elements in Factor 1 can be attributed to two processes: (a) mixing of the groundwater with the seawater and (b) dissolution and leaching of terrestrial salts present in the Neogene and Quaternary deposits of the Oropos–Kalamos basin. This factor expresses the total salt concentration of the groundwater samples, which is determined by these ions. Factor 1 may be referred to as “salinity factor”. The groundwater sample collected from the Ag.Apostoloi area (sampling site: S1) revealed the heaviest load of the above elements because of its mixing with seawater (Fig. 8). Groundwater samples collected in the area lying between Oropos, Nea Palatia, Mavrosouvala and Markopoulo have the lowest load of the above elements.

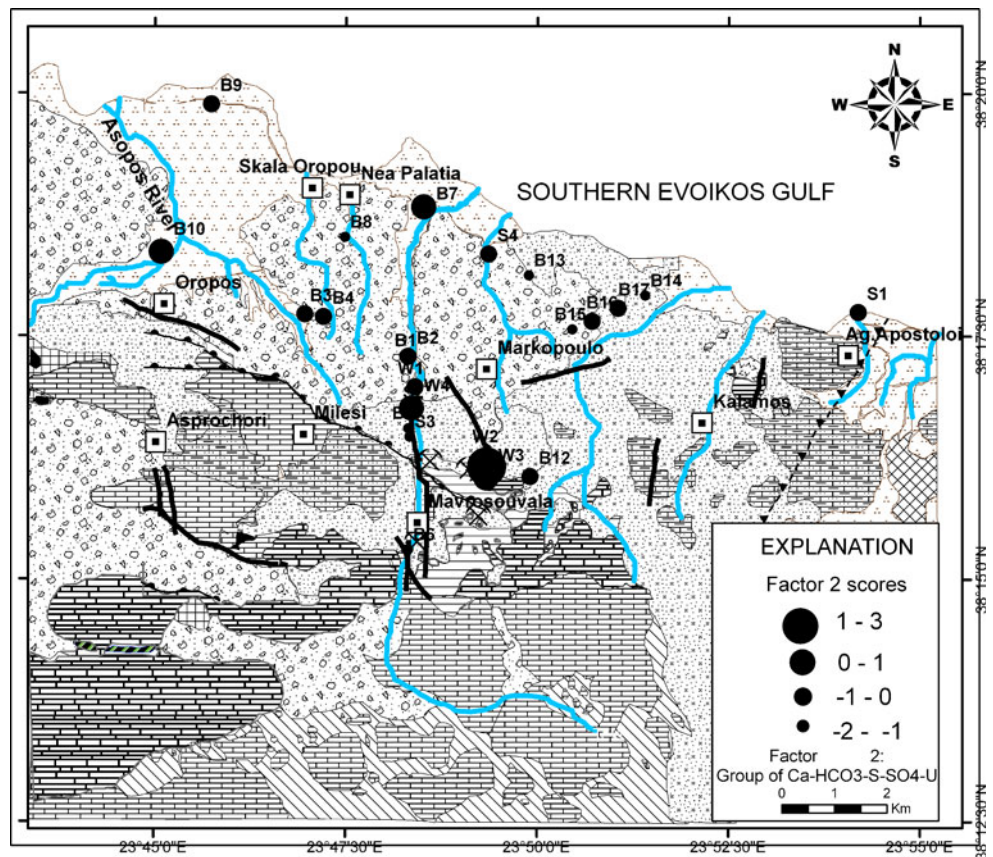
Factor 2, which explains 14.69% of total variance, has high positive loadings ($>+0.744$) on Ca, S, SO_4 and U, and

moderate positive loading ($+0.567$) on HCO_3^- (Table 2). The close relationships between Ca– SO_4 and Ca– HCO_3^- can be attributed to the minerals anhydrite and calcite, respectively, which are present in the lignite intercalations and Neogene sediments. The presence of elevated Ca, S, SO_4 and U concentrations can also be attributed to the dissolution of lignite intercalations. Therefore, Factor 2 is related mainly to natural sources.

The inclusion of U in Factor 2 bears further discussion. According to the measured pH conditions, U can occur mainly as a carbonate ion complex $\text{UO}_2(\text{CO}_3)_2^{2-}$ and $\text{UO}_2(\text{CO}_3)_3^{4-}$ (Gascoyne 1989).

The hypothesis that U concentrations higher than $5 \mu\text{g L}^{-1}$ are the result of an enrichment mechanism implies many or all of the following circumstances: (a) uranium enrichment of lignite intercalations and Neogene deposits due to the dissolution of volcanosedimentary formations and past geothermal activity; (b) occurrence of U in lignite intercalations in the +4 oxidation state. Uranium is immobile at that state, at low temperature and pressures (Skeppstrom and Oloffson 2007); (c) an oxidizing environment (shallow aquifer with groundwater contains an appreciable amount of dissolved oxygen); (d) uranium is oxidized to the more mobile state +6, gets into solution and is transported together with the

Fig. 9 Graduated symbol plots of Factor 2 scores in comparison with geology



groundwater as UO_2^{2+} ; and/or (e) the UO_2^{2+} ions form complexes with existing ions in Oropos–Kalamos groundwater such as HCO_3^- and SO_4^{2-} . Therefore, Factor 2 may be termed a “U enrichment mechanism”. The higher positive Factor 2 scores are observed in the area close to the abandoned lignite mines, especially in the aquifer that is in contact with lignite intercalations demonstrating Factor 2 association with lignite intercalations (Fig. 9).

Factor 3 shows a variance of 14.69% and has high positive loadings ($>+0.898$) for Cr^{6+} and Cr_{tot} and moderate positive loading for NO_3 ($+0.509$) and Si ($+0.655$) (Table 2). This factor explains the redox transformation of Cr^{3+} into Cr^{6+} or vice versa, which can only take place in the presence of another redox couple that accepts or donates the three necessary electrons. According to Richard and Bourg (1991), one of the redox couples that controls chromium speciation in natural aquatic environments is the NO_2/NO_3 couple. Significantly, the higher positive Factor 3 values are mainly observed in the area lying between Oropos and Markopoulo, which is characterized by cultivated areas and intensive agricultural practices (Fig. 10). This suggests that Factor 3 is associated with agricultural inputs to groundwater and that nitrate (NO_3) plays an important role in controlling Cr speciation. Thus, Factor 3 may be termed a “Cr redox couple factor”.

Factor 4, accounting for only 7.97% of the total variance, is a factor with high positive loadings for As ($+0.780$), Mn ($+0.889$) and moderate positive loadings ($>+0.509$) for Ni, Rb and Si (Table 2). The higher positive scores are recorded in the area between Markopoulo, Mavrosouvala and Oropos, demonstrating an association of Factor 4 with both lignite intercalations and intensive agricultural activities (Fig. 11). Thus, the positive loadings of As, Mn and Ni on Factor 4 appear to be related to two factors: (a) natural sources, such as leaching from the lignite intercalations, and (b) anthropogenic sources, such as leaching from the lignite tailings and application of fertilizers and agricultural chemicals (Alexakis 2008; Alexakis 2010; Kabata-Pendias and Kabata 1995; Shomar et al. 2005). Arsenic, Mn and Ni could occur as adsorbed species in lignite intercalations, and lignite mining works are a common anthropogenic source of Cd, Co, Cr, Cu, Fe, Hg, Mn, Ni, Pb, SO_4^{2-} and Zn contamination worldwide (Dimitrakopoulos et al. 2007; Kabata-Pendias 1995; Khan et al. 2005; Fang et al. 2003). Furthermore, the application of agricultural chemicals (pesticides, herbicides and fungicides) and fertilizers can lead to As and Mn contamination (Shomar et al. 2005; Alloway 1995). In light of these associations, Factor 4 may be termed an “As–Mn–Ni contamination” factor.

Fig. 10 Graduated symbol plots of Factor 3 scores in comparison with geology

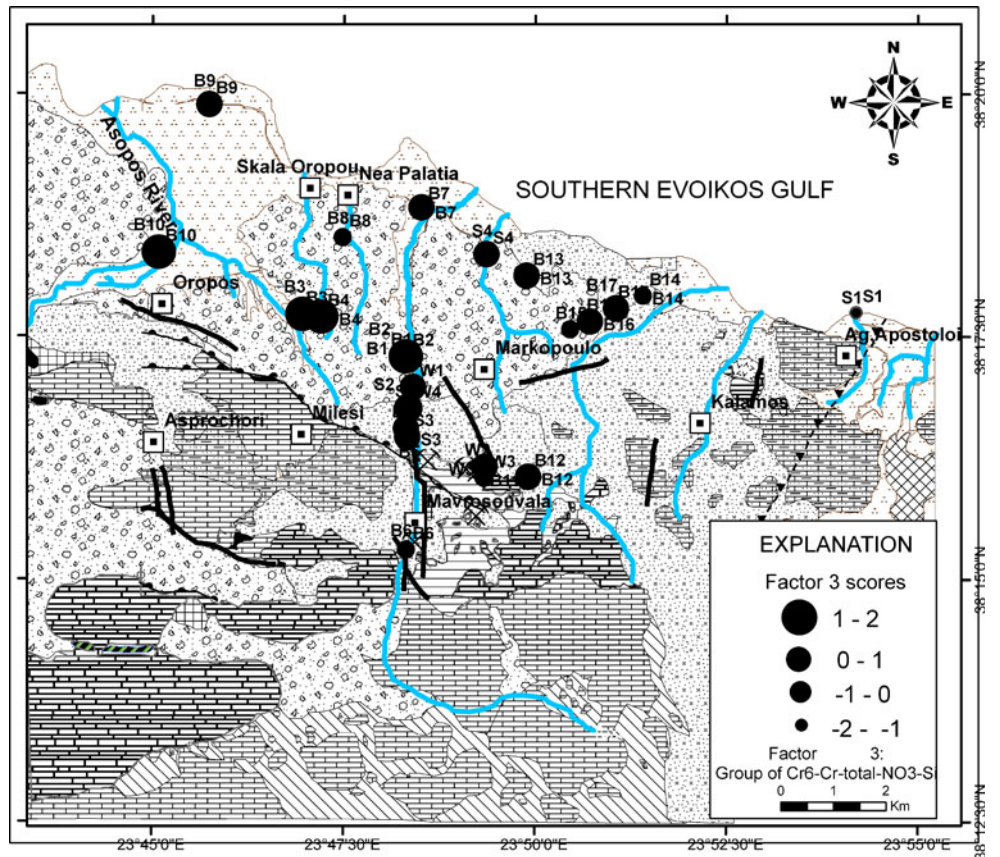
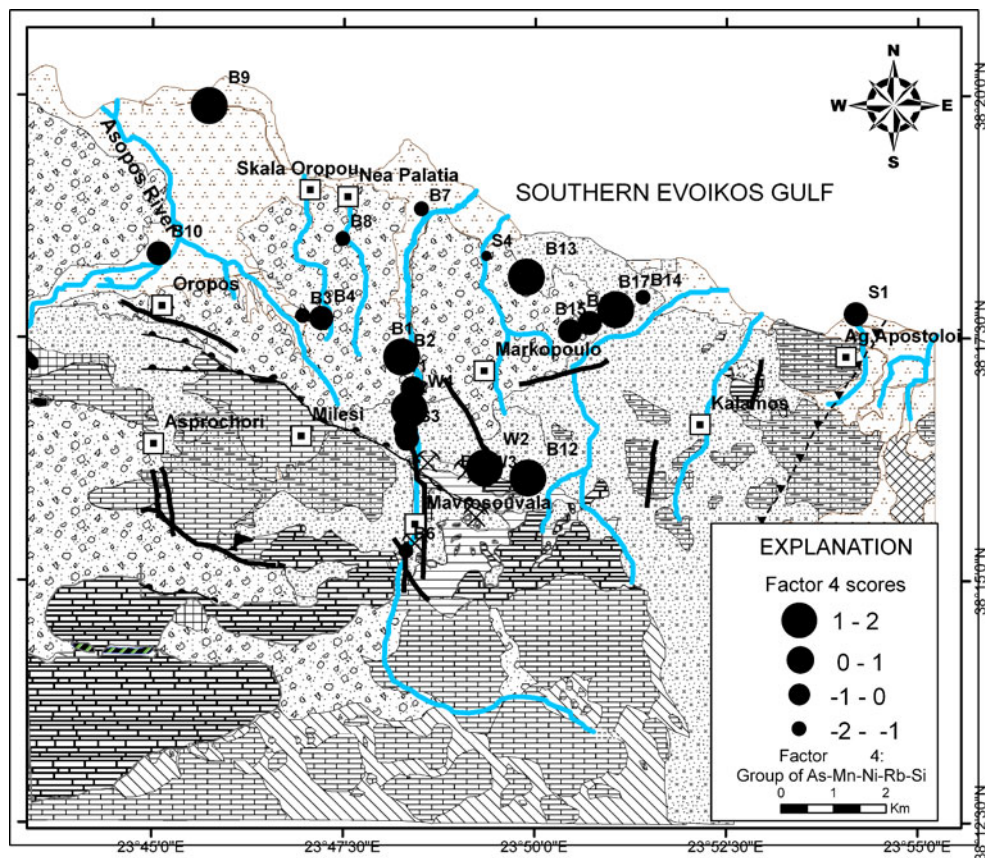


Fig. 11 Graduated symbol plots of Factor 4 scores in comparison with geology



Conclusions

Groundwater quality in the Oropos–Kalamos basin has been found to belong to five types: Ca–HCO₃, Mg–HCO₃, Na–Cl, Mg–Cl and Ca–Cl. The main minerals present in the water-bearing formations of this region are calcite (CaCO₃), aragonite (CaCO₃), anhydrite (CaSO₄), dolomite (CaMg(HCO₃)₂), gypsum (CaSO₄·2H₂O) and magnesite (MgCO₃). Groundwaters in the study area are saturated with respect to calcite, aragonite, magnesite and dolomite and unsaturated with respect to gypsum and anhydrite. Therefore, there is a potential for Ca²⁺ and SO₄²⁻ concentrations to increase as a result of gypsum and anhydrite dissolution.

This study found concentrations of As, Cl, Fe, Mn, Na, NH₄⁺, Ni, Pb, Se and SO₄²⁻ in groundwater of the Oropos–Kalamos basin that exceeded the European Community (EC) health-based drinking water guidelines, and 8 of the 25 sampling sites yielded water that was not suitable for irrigation purpose. Elevated concentrations of U and V were also measured, but these elements were not included in the EC table of PVs. Given the possible toxic effects of U and V to humans, it is important that EC consider drinking water standards for these elements.

GIS analysis was found to be a very useful tool in the evaluation of groundwater quality within the Oropos–Kalamos basin. Using this approach, natural sources (such as past geothermal activity, terrestrial salts, volcanic sedimentary formations, lignite intercalations, ultrabasic rock masses and chromiferous iron ores) were identified for the As, B, Ca, Cl, Cr⁶⁺, Cr_{total}, HCO₃⁻, K, Mg, Mn, Na, Ni, Rb, S, Si, SO₄²⁻, V and U in groundwater. High As, U and V concentrations are associated with the distribution of marly limestones, travertines and marly formations with lignite intercalations; and high Cr_{total} and Cr⁶⁺ concentrations are derived from the weathering products of ultrabasic rock masses in the presence of the NO₂/NO₃ redox couple, which comes from nitrate fertilizers applied in cultivated areas. In addition to NO₃⁻, the application of fertilizers and agricultural chemicals influences the occurrences of As, Mn and Ni. A spatial relationship was also found between the occurrences of B, Cl, K, Mg, Na, Rb and V and seawater intrusion.

Factor analysis of the Oropos–Kalamos groundwater quality data set, which explains 77.41% of the total variability, showed the presence of four groups of inter-correlated water quality parameters. Factor 1 (the salinity factor), which includes B, Cl, K, Mg, Na, Rb and V, is related to natural sources (the mixing of groundwater with the seawater and the dissolution of terrestrial salts present in the Neogene and Quaternary deposits). Factor 2 (the U enrichment factor) is an association between Ca, S, SO₄²⁻, U and HCO₃⁻, which are derived from both natural (lignite

intercalations, anhydrite, calcite, geothermal activity) and anthropogenic sources. The association of Cr⁶⁺, Cr_{total}, NO₃ and Si (Factor 3, the Cr redox couple factor) is also related to both natural (ultrabasic rock masses and ultrabasic fragments within Neogene–Quaternary deposits) and anthropogenic (nitrate fertilizers) sources. This factor explains the redox transformation of Cr³⁺ into Cr⁶⁺, or vice versa, which takes place in the presence of the NO₂/NO₃ redox couple derived from nitrate fertilizers applied in cultivated areas. Factor 4 includes the grouping of As, Mn and Ni, which are leached from naturally occurring lignite intercalations and from lignite tailings or fertilizers.

Acknowledgments We thank N. Voutsis and S. Peppas for the assistance rendered during the fieldwork of this study. We would like to thank the staff of the Department of Economic Geology and Geochemistry, National and Kapodistrian University of Athens, for cooperation during the chromium analyses by using AAS. The authors are thankful to the anonymous reviewer for giving valuable suggestions for improving the quality of the paper.

References

- Alexakis D (2008) Geochemistry of stream sediments as a tool for assessing contamination by arsenic, chromium and other toxic elements: East Attica region, Greece. *Eur Water* 21(22):57–72
- Alexakis D (2010) Diagnosis of stream sediment quality and assessment of toxic element contamination sources in East Attica, Greece. *Environ Earth Sci*. doi:10.1007/s12665-010-0807-9
- Alexakis D, Kelepertsis A (1998) The relationship between the chemical composition-quality of groundwaters and the geological environment in the East Attiki area, Greece. *Miner Wealth* 109:9–20
- Alloway BJ (1995) Heavy metals in soil, 2nd edn. Blackie Academic Professional, An imprint of Chapman and Hall, London
- Arumugam K, Elangovan K (2009) Hydrochemical characteristics and groundwater quality assessment in Tirupur Region, Coimbatore District, Tamil Nadu, India. *Environ Geol* 58:1509–1520. doi:10.1007/s00254-008-1652-y
- Ball JW, Izbicki JA (2004) Occurrence of hexavalent chromium in groundwater in the western Mojave Desert, California. *Appl Geochem* 19:1123–1135
- Ball JW, McCleskey RB (2003) A new cation-exchange method for accurate field speciation of hexavalent chromium. *Talanta* 61:305–313
- CCME (1999) Canadian Council of Minister of the Environment. Canadian Water Quality Guidelines for the Protection of Agricultural Water Uses. Canadian Environmental Quality Guidelines. Pub.No. T/528
- Chatziapostolou A, Kalaitzidis S, Papazisimou S, Christanis K, Vagias D (2006) Mode of occurrence of trace elements in the Pellana lignite (SE Peloponnese, Greece). *Int J Coal Geol* 65:3–16
- Davis JC (1986) Statistics and data analysis in geology. Wiley, New York
- Dimitrakopoulos D, Vassiliou E, Founda M (2007) Impacts of mining activities on water resources to Megalopolis lignite district area. *Geophysical Research Abstracts*, Vol9.11028. SRef-ID (2007) 1607-7962/gra/EGU2007-A-11028. European Geosciences Union 2007

- EC (1998) Council Directive 98/83/EC Directive of the European Parliament on the quality of water intended for human consumption. The European Parliament and the Council of the European Union. Off J L 330
- Espinosa E, Aurora Armienta M, Cruz O, Aguayo A, Ceniceros N (2009) Geochemical distribution of arsenic, cadmium, lead and zinc in river sediments affected by tailings in Zimapan, a historical polymetallic mining zone of Mexico. *Environ Geol* 58:1467–1477. doi:10.1007/s00254-008-1649-6
- Fang WX, Huang ZY, Wu PW (2003) Contamination of the environmental ecosystems by trace elements from mining activities of Badao bone coal mine in China. *Environ Geol* 44:373–378
- Fantoni D, Brozzo G, Canepa M, Cipolli F, Marini L, Ottonello G, Zuccolini M (2002) Natural hexavalent chromium in groundwaters interacting with ophiolitic rocks. *Environ Geology* 42:871–882
- Fehdi Ch, Aek Rouabhia, Baali F, Boudoukha A (2009) The hydrogeochemical characterization of Morsott-El Aouinet aquifer, Northeastern Algeria. *Environ Geol* 58:1611–1620. doi:10.1007/s00254-008-1667-4
- Gascoyne (1989) High levels of uranium and radium in groundwaters at Canada's Underground Research Laboratory, Lac du Bonnet, Manitoba, Canada. *Appl Geochem* 4:577–591
- Hoell K (1979) Wasser: Untersuchung, Beurteilung, Aufbereitung, Chemie, Bakteriologie, Virologie, Biologie. Walter de Gruyter, Berlin
- IGME (2000) Eretria sheet. Geological Map 1:50,000. Department of Geological Maps. Institute of Geology and Mineral Exploration, Athens 2000
- Kabata-Pendias A (1995) Agricultural problems related to excessive trace metal contents of soils. In: Salomons W, Forstner U, Mader P (eds) Heavy metals: problems and solutions. Springer, Berlin, pp 3–18
- Kabata-Pendias A, Pendias H (1995) Trace elements in soils and plants. CRC press, Inc, Boca Raton
- Kehagia K, Koukoulidou V, Bratakos S, Seferlis S, Tzoumerkas F, Potiriadis C (2007) Radioactivity monitoring in drinking water of Attica, Greece. *Desalination* 213:98–103
- Kelepertsis A, Alexakis D, Skordas K (2006) Arsenic, antimony and other toxic elements in the drinking water of Eastern Thessaly in Greece and its possible effects on human health. *Env Geol* 50:76–84. doi:10.1007/s00254-006-0188-2
- Khan R, Israili SH, Ahmad H, Mohan A (2005) Heavy metal pollution assessment in surface water bodies and its suitability for irrigation around the Neyevli Lignite Mines and Associated Industrial Complex, Tamil Nadu, India. *Mine Water Environ* 24:155–161
- Lambrakis N (2006) Multicomponent heterovalent chromatography in aquifers. Modelling salinization and freshening phenomena in field conditions. *J Hydrol* 323:230–243
- Liou T-S, Lu H-Y, Lin C-K, Lin W, Chang Y-T, Chien J-M, Chen W-F (2009) Geochemical investigation of groundwater in a Granitic Island: a case study from Kinmen Island, Taiwan. *Environ Geol* 58:1575–1585. doi:10.1007/s00254-008-1664-7
- Nalbantis I, Tsakiris G (2009) Assessment of hydrological drought revisited. *Water Resour Manag* 23:881–897
- Orloff KG, Mistry K, Charp P, Metcalf S, Marino R, Shelly T, Melaro E, Danohoe A, Jones R (2004) Human exposure to uranium in groundwater. *Environ Res* 94:319–326
- Papanikolaou DJ, Mariolakos ID, Lekkas EL, Lozios SG (1988) Morphotectonic observations on the Asopos basin and the Coastal zone of Oropos. Contribution to the Neotectonics of Northern Attica. *Bulletin Geological Society, Greece*, pp 251–267
- Pe-Piper G, Piper D (2002) The igneous rocks of Greece. The anatomy of an orogen. *Beitrag zur regionalen geologie der erde*. Band 30. Berlin-Stuttgart
- Richard FC, Bourg AC (1991) Aqueous geochemistry of chromium: a review. *Wat. Res.* 25(7):807–816
- Robles-Camacho J, Armienta MA (2000) Natural chromium contamination of groundwater at Leon Valley, Mexico. *J Geoch Explor* 68:167–181
- Shomar BH, Muller G, Yahya A (2005) Geochemical features of topsoils in the Gaza Strip: natural occurrence and anthropogenic inputs. *Environ Res* 98:372–382
- Simsek C (2008) Assessment of natural radioactivity in aquifer medium bearing uranium ores in Koprubasi, Turkey. *Environ Geol* 55:1637–1646. doi:10.1007/s00254-007-1113-z
- Singh P, Rana NP, Azam A, Naqvi AH, Srivastava DS (1996) Levels of uranium in waters from some Indian cities determined by fission track analysis. *Radiation Measurements* 26(5):683–687
- Skeppstrom K, Olofsson B (2007) Uranium and radon in groundwater. an overview of the problem. *Eur Water* 17(18):51–62
- Stamatis G, Gartzos E (1999) The silica supersaturated waters of northern Evia and eastern central Greece. *Hydrol Process* 13:2833–2845
- Stamatis G, Lambrakis N, Alexakis D, Zagana E (2006) Groundwater quality in eastern Attica (Greece). *Hydrolol Process* 20:2803–2818
- Tsakiris G, Spiliotis M, Paritsis S, Alexakis D (2009) Assessing the water potential of karstic saline springs by applying a fuzzy approach: the case of Almyros (Heraklion, Crete). *Desalination* 237:54–64
- Venkataraman BV, Sudha S (2005) Vanadium Toxicity. *Asian J Exp Sci* 2:127–134
- Voreadis G (1952) The tertiary lignite basin of Malakasa-Oropos. *Geol Geophys Sur* 2: 141–180
- WHO (2004) Guidelines for drinking water quality, vol 1. World Health Organisation, Geneva, pp 1–494
- Zamora ML, Tracy BL, Zielinski JM, Meyerhof DP, Moss MA (1998) Chronic ingestion of uranium in drinking water: a study of kidney bioeffects in humans. *Toxicol Sci* 43:68–77